Supporting Information

"Development of Amidine-Based Sphingosine Kinase 1 Nanomolar Inhibitors and Reduction of Sphingosine 1-Phosphate in Human Leukemia Cells"

Andrew J. Kennedy,[,1] Thomas P. Mathews,[1,2] Yugesh Kharel,[2] Saundra D. Field,[1] Morgan L. Moyer,[1] James E. East,[1] Joseph D. Houck,[1] Kevin R. Lynch,[2] and Timothy L. Macdonald[1,2]*

[1]University of Virginia Department of Chemistry, McCormick Road, Charlottesville, VA 22904, [2]University of Virginia Department of Pharmacology, Jefferson Park Avenue, Charlottesville, VA 22904

Table of Contents

SphK1 Homology Model. A homology model of SphK1 was produced using the known crystal structure of DGKB (PDB:2QV7) as a template.[1] The sequence alignment was produced using the blosum62 tree-base algorithm[2] present in the Molecular Operating Environment (MOE) software[3] and then manually adjusted (Figure SI-1). The two large areas of the primary SphK1 sequence that do not correspond with the structure of DGKB were deleted. The sequence containing Ser225 and responsible for extracellular-signal-regulated kinase (ERK) recognition[4] between and including Arg209 and Trp249, and the 28 amino acid sequence that recognizes sphingosine between and including Trp171 and Leu198 were removed and left as an open gap. All waters were removed from the crystal structure, but ADP was kept. The ADP was converted to ATP by the addition of a third phosphate and a Mg^{2+} ion was manually added to chelate ATP in a structurally similar fashion as reported in other related crystal structures.[5, 6] The ATP•Mg^{2+} complex was then fixed and the DGKB structure allowed to minimize in an Amber 99 force field. The SphK1 homolog, lacking the 28 amino acids relevant to sphingosine binding, was then produced by generating 20 crude models, using the standard parameters, and minimized in an Amber 99 force field. The models were ranked by stability, with the lowest energy homolog being advanced to the next stage of design. This partial SphK1 homolog then had its sphingosine binding sequence reincorporated, and a full SphK1 homolog was produced form this partial homolog. With the ATP•Mg^{2+} complex still fixed and bound to the partial SphK1 homolog, 64 theoretic loops, turns, and helices were generated, using the standard homology model building parameters, to close the gap in the SphK1 sequence and structure produced by the deletion of these 28 amino acids. The set of 64 SphK homologs was then minimized in an Amber 99 force

field and judged both on overall stability and the ability for the pocket to accommodate sphingosine. The ATP•Mg^{2+} complex was then unfixed and allowed to minimize in an Amber 99 force field with the unfixed protein to yield the SphK1 homolog used in this publication.

```
DGKB   MRKRARIIYNPTSGKEQFKRELPDALIKLEKAG•YETSAYATEKIGDATLEAERAMHENYDVL 62
SphK1  RPCRVLVLLNPRGGKGKALQLFRSHVQPLLAEAEISFTLMLTERRNHARELVRSEELGRWDAL 75
          *: ::.**..** :  : : . :  *   : .  :...**:  .*.  .:.  . .:*:*
DGKB   IAAGGDGTLNEVVNGIAEKPN•••••RPKLGVIPMGTVNDFGRAL•HIPN•DIMGALDVIIE• 117
SphK1  VVMSGDGLMHEVVNGLMERPDWETAIQKPLCSLPAGSGNALAASLNHYAGYEQVTNEDLLTNC 138
       :: .***.:.*****: *:*:     :  *. :* *:.* :: :* *:   : .   *:: :
DGKB   ••••••GHSTKVDIGKMNNRYFINLAAGGQ•••GPFA••••••••••LPQMK•••••••AVD 177
SphK1  TLLLCRRLLSPMNLLSLHTASGLRLFSVLSLAWGFIADVDLESEKYRRLGEMRFTLGTFLRLA 201
              . : .::  :.  : ::* .      * :*           *  *:        :
DGKB   LRIEYDG••••••••••••••••••••••••••••••••••••••••NVFQGEALLFFLGLT 199
SphK1  ALRTYRGRLAYLPVGRVGSKTPASPVVVQQGPVDAHLVPLEEPVPSHWTVVPDEDFVLVLALL 264
       .  .*:*                                      .*:  * ::::*:*:
DGKB   NSMAGFEKLV•PDAKLDDGYFTLIIVEKS•NLAELGHIMTLASRGEHTKH••PKVIYEKAKAI 258
SphK1  HSHLGSEMFAAPMGRCAAGVMHLFYVRAGVSRAMLLRLFLAMEKGRHMEYECPYLVYVPVVAF 327
       .*..* * :: * ::   * .:*::*: :   * * ::..  ::*:* ::  *.::*  : *:
DGKB   NISSFTD•LQLNVDGEYGGKLPANFLNLERHIDVFAPNDIVNEELINNDHVDDNL         313
SphK1  RLEPKDGKGVFAVDGELMVSEAVQGQVHPNYFWMVSGCVEPPPSWKPQQ               376
       .::  :  . : ****. .   ::.  . .::  ::       :
```

Figure SI-1. Sequence Alignment of SphK1 and DGKB.

Inhibitor Docking. Compounds **1**, **2**, **36a**, and **36b** were initially docked into the homology model of SphK using the docking function present in the MOE[3] software package. The molecules were placed using the Triangle Matcher algorithm into the sphingosine binding pocket in a fixed environment, allowed to minimize in the MMFF94x force field, and scored using the London ΔG function until 100 unequivalent crude docking conformations were obtained. London ΔG predicts the energy of binding, so the conformer in the lowest score was taken on to a more rigorous conformational search. Using a systematic conformational search, each rotatable bond was rotated 120

degrees to generate a library of conformers. Each member of this library was then docked without ligand minimization and scored using the London ΔG function. The 500 conformers with the lowest scores were allowed to minimize in the fixed pocket, and then minimized with the pocket unfixed using the MMFF94x force field.

The London ΔG scoring function was not sufficient by itself to yield scores correlative to activity. This is because London ΔG estimates the energy of binding and the entropy associated with locking the compound into a given conformation. It does not take into account conformational strain that the inhibitor must pay for in adopting its active form nor judge solubility effects, such as a lowered active concentration for highly lipophilic compounds due to self-aggregation. As to correct for these omitted factors, the scoring function chosen was a multivariable regression that weighs a compound's London ΔG score, the energy difference between the inhibitors active conformation and its minimum energy conformation, and its deviation from the empirically-estimated ideal Clog P of 4.2. These final conformers were then scored using the empirical scoring function (1). Where π is the hydrophobicity constant (2) from the Hansch linear free-energy equation and ligand strain is defined as the ΔG (kcal/mol) between the bound conformation of the ligand and the global minimum of the ligand as determined in a MMFF94x force field with a dielectric constant set to 80. Multivariable regression analysis then systematically varies the weight each variable contributes to the overall score of the inhibitor until a global maximum for the model's R^2 value is achieved. In this way, the exact formula for the scoring function evolves with every new inhibitor docked, synthesized and tested, and the scoring function (1) was determined from the inhibitors in this study. For all other docked compounds, a crude binding conformation

was generated from compounds **1**, **2**, **36a**, or **36b**, and was then taken on to the stated systematic conformational search and docking protocol.

$$pK_I \text{ (predicted)} = -3.78 - (0.56 \times \text{London } \Delta G) + (0.21 \times -\pi^2) - (0.33 \times \text{ligand strain}) \quad (1)$$

$$\pi = 4.2 - \text{Clog } P^7 \quad (2)$$

Scoring function (1) was able to accurately rationalize ideal tail lengths, head group activity, and terminal ring substitution effects. Figure SI-2 shows the correlation between the docked library's predicted K_I values (Table SI-1) and measured K_I values, and the model's linear relationships of $R^2 = 0.77$. The synthesis and SAR of this library was critical for deriving these relationships, since the coefficients within the multivariable scoring function are all empirically determined from this data set.

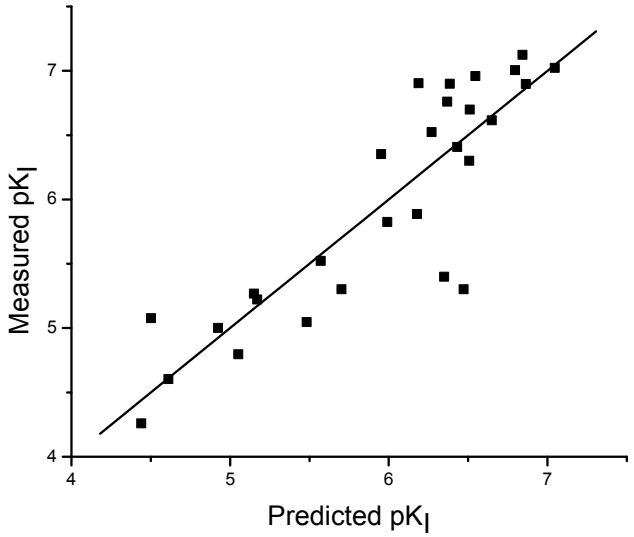

Figure SI-2. Docking studies of Amidine Library with SphK1. Measured pK_I versus predicted pK_I ($R^2 = 0.77$).

Table SI-1. Amidine-Based Inhibitor Docking Results

Compound	SphK1 K_i (μM)	London ΔG	Ligand Strain	CLog P	Predicted pK_i	Measured pK_i	Z score
Compound 9 from ref 1	55	-16.94	1.0	1.82	4.4	4.3	0.44
1 C8	25	-17.02	1.0	1.97	4.6	4.6	0.02
1 C10	5	-18.01	1.0	2.75	5.7	5.3	0.98
1 C12	0.2	-18.95	1.0	3.53	6.5	6.7	0.46
1 C14	10	-19.78	7.4	4.31	4.9	5.0	0.18
2 C10	3	-17.43	1.0	3.20	5.6	5.5	0.12
2 C12	0.3	-18.44	1.0	3.99	6.3	6.5	0.61
2 C14	8.4	-19.21	7.4	4.77	4.5	5.1	1.40
4a	6	-17.69	2.0	2.70	5.2	5.2	0.12
4b	5.4	-18.57	4.5	3.48	5.2	5.3	0.29
4c	9	-19.60	5.4	4.26	5.5	5.0	1.06
9a	5	-19.47	2.0	3.50	6.5	5.3	2.85
9b	0.392	-18.95	1.0	3.22	6.4	6.4	0.06
9c	0.243	-19.17	1.0	3.61	6.7	6.6	0.09
14a	0.5	-19.44	2.0	4.04	6.5	6.3	0.50
14b	1.3	-18.90	2.0	3.65	6.2	5.9	0.71
19a	0.111	-19.54	1.0	2.71	6.5	7.0	1.00
19b	0.445	-18.91	1.0	2.32	6.0	6.4	0.97
23a	0.127	-19.76	1.0	3.15	6.9	6.9	0.08
23b	0.174	-19.18	1.0	2.77	6.4	6.8	0.95
23c	1.3	-18.92	1.0	2.38	6.0	5.9	0.40
26	0.095	-20.30	1.0	2.86	7.0	7.0	0.06
30	4	-18.97	1.0	3.20	5.5	5.4	0.12
36a	0.125	-18.30	1.0	3.87	6.2	6.9	1.74
36b	16	-18.59	5.1	3.87	5.1	4.8	0.62
38	0.075	-19.55	1.0	3.50	6.8	7.1	0.69
40	0.099	-19.53	1.0	3.20	6.8	7.0	0.51
47	0.126	-18.88	1.0	4.65	6.4	6.9	1.25

***In Silico* Linker Screen.** From the docking conformation of compounds **19a**, **26**, and **38** the alkyl chain between the amide bond and the cyclohexyl tail was deleted. Linkers between the head and tail fragments were then manually bridged by the addition of benzenes (para and meta substituted), five and six membered heterocycles, saturated rings, fused rings, and alkyl spacers in varying order. These theoretical structures were then minimized in the pocket in a MMFF94x force field and scored using function (1).

Clog P Comparison to HPLC Retention Time (t_R). In order to evaluate how well Clog P predicts water solubility for amidine containing inhibitors, Clog P values were correlated with the determined retention times of the inhibitors using reverse-phase HPLC. Figure SI-3 shows the correlation between retention time (t_R) and Clog P with an $R^2 = 0.71$. The left figure represents the library excluding compound **53**, since its Clog P value does not take into account its protonation state. The right figure includes compound **53** as an outlier (red dot), validating the hypothesis that its underperformance *in vitro* was due to a misjudgment of its water solubility.

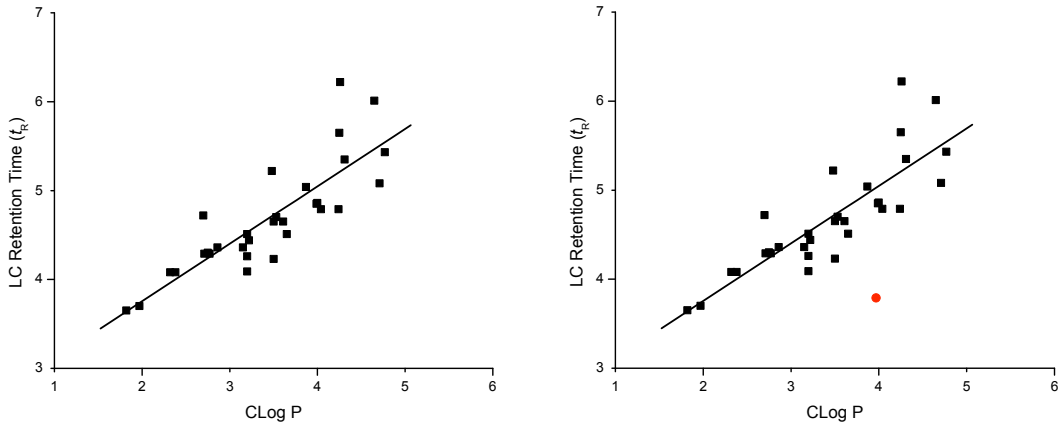

Figure SI-3. (Left) The correlation between LC retention time and Clog P of the amidine-based SphK inhibitor library. ($R^2 = 0.71$) (Right) Includes compound **53** (red dot), which contains an imidazole with a Clog P not representative of its true water solubility.

Scheme SI-1. Synthesis of **30**

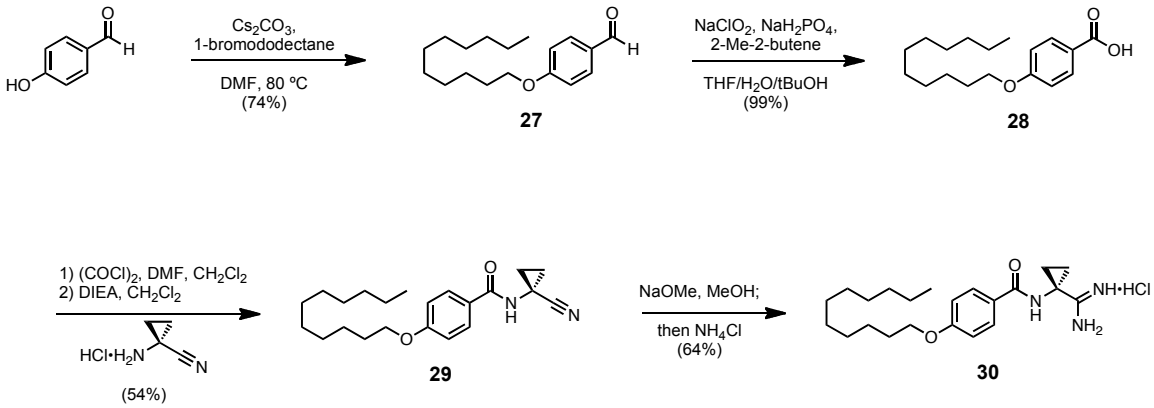

Scheme SI-2. Synthesis of **47**

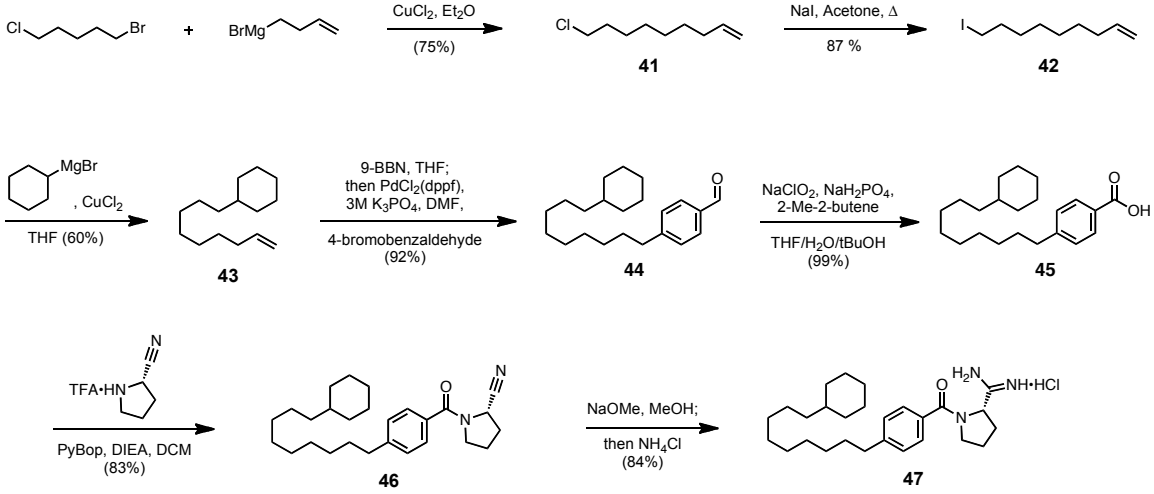

Experimental Data for Compounds 30 and 47

4-(undecyloxy)benzaldehyde (27). To a stirring solution of 4-hydroxybenzaldehyde (1.0 g, 8.2 mmol) in DMF (0.6 M), the alkyl bromide (1.5 eq.) and cesium carbonate (2 eq.) were added and the reaction mixture was heated to 65 ºC. Once complete by TLC analysis, the reaction was cooled and the salt removed by filtration through a course-fritted funnel. The supernatant was diluted with EtOAc (150 mL) and extracted 3x with neat water (30 mL). The organic layer was dried over magnesium sulfate and the solvent removed under reduced pressure to afford a tan oil. The product was purified by flash column chromatography. 74%. White solid. R_f = 0.70 (10% EtOAc in hexanes; Seebach's Dip). ^{1}H NMR (300 MHz, $CDCl_3$) δ 9.87 (s, 1H), 7.82 (d, *J* = 8.8 Hz, 2H), 6.99 (d, *J* = 8.8 Hz, 2H), 4.03 (t, *J* = 6.5 Hz, 2H), 1.76 – 1.87 (m, 2H), 1.26 – 1.48 (m, 16H), 0.88 (t, *J* = 6.7 Hz, 3H); ^{13}C NMR (75 MHz, $CDCl_3$) δ 191.0, 164.4, 132.1, 129.8, 114.9, 68.6, 34.3, 32.1, 29.7, 29.6, 29.2, 29.0, 28.3, 26.1, 22.8, 14.3.

***N*-(1-cyanocyclopropyl)-4-(undecyloxy)benzamide (29).** General procedure K was used to convert **27** (1.7 g, 6.5 mmol) to is corresponding carboxylic acid **28**, which was taken on to the next reaction crude. General procedure I was then used to convert the crude carboxylic acid to its acid chloride and was used immediately after purification. General procedure M was used to couple the acid chloride and 1-amino-1-cyclopropanecarbonitirle to yield the title compound. 54% over 3 steps. While solid. R_f = 0.46 (40% EtOAc in hexanes; Seebach's Dip). ^{1}H NMR (500 MHz, $CDCl_3$) δ 7.92 (s, 1H), 7.71 (d, *J* = 8.6 Hz, 2H), 6.90 (d, *J* = 8.6 Hz, 2H), 3.98 (t, *J* = 6.6 Hz, 2H), 1.79 (quin., *J* = 5.0 Hz, 2H), 1.62 (m, 2H), 1.45 (quin., *J* = 5.0 Hz, 2H), 1.35 (dd, *J* = 9.0 Hz, 6.1 Hz, 2H), 1.20 – 1.32 (m, 14H), 0.88 (t, *J* = 6.9 Hz, 3H); ^{13}C NMR (125 MHz, $CDCl_3$)

δ 168.2, 162.8, 129.6, 124.8, 120.8, 114.6, 68.5, 32.2, 29.90, 29.87, 29.68, 29.65, 29.4, 26.3, 23.0, 21.2, 17.2, 14.4.

***N*-(1-carbamimidoylcyclopropyl)-4-(undecyloxy)benzamide hydrochloride (30).** General procedure A was used to convert **29** (100 mg, 0.27 mmol) to the title compound. 64%. White solid. ^{1}H NMR (500 MHz, CD_3OD) δ 7.88 (d, *J* = 8.6 Hz, 2H), 6.97 (d, *J* = 8.6 Hz, 2H), 4.03 (t, *J* = 6.3 Hz, 2H), 1.81 – 1.74 (m, 4H), 1.56 – 1.21 (m, 18H), 0.90 (t, *J* = 6.7 Hz, 3H); ^{13}C NMR (125 MHz, CD_3OD) δ 174.8, 171.7, 164.9, 131.68, 131.4, 126.9, 116.0, 70.1, 34.9, 33.9, 31.6, 31.4, 31.1, 28.0, 24.6, 20.4, 17.9, 15.3. LCMS: t_R = 4.09; m/z = 374.3. HRMS m/z calc. for $C_{22}H_{36}N_3O_2$ (M+H), 374.2808; found, 374.2810.

9-chlorononon-1-ene (41). General procedure F was used to couple 1-bromo-5-chloropentane (2.00 mL, 15.2 mmol) and 3-butenylmagnesium bromide (2 M solution in THF) to yield the title compound. 75%. Clear and colorless oil. R_f = 0.88 (hexanes; $KMnO_4$). ^{1}H NMR (500 MHz, $CDCl_3$) δ 5.92 – 5.63 (m, 1H), 5.12 – 4.77 (m, 2H), 3.51 (t, *J* = 6.7 Hz, 2H), 2.05 (td, *J* = 6.8, 1.0 Hz, 2H), 1.83 – 1.69 (m, 2H), 1.51 – 1.16 (m, 10H). ^{13}C NMR (126 MHz, $CDCl_3$) δ 138.85, 114.20, 44.90, 33.73, 32.63, 28.93, 28.79, 28.74, 26.83.

9-iodononon-1-ene (42). To a solution of **41** (1.80 g, 11.4 mmol) in acetone (0.57 M) was added sodium iodide and heated to reflux for 12 h. The reaction was then evaporated to dryness and purified by flash chromatography. 87%. Clear and colorless oil. R_f = 0.85 (hexanes; $KMnO_4$). ^{1}H NMR (500 MHz, $CDCl_3$) δ 5.92 – 5.65 (m, 1H), 5.12 – 4.76 (m, 2H), 3.17 (t, *J* = 8.0 Hz, 2H), 2.10 – 1.91 (m, 2H), 1.89 – 1.71 (m, 2H), 1.46 – 1.11 (m,

10H). ^{13}C NMR (126 MHz, $CDCl_3$) δ 138.88, 114.31, 33.75, 33.55, 30.48, 28.91, 28.82, 28.42, 7.11.

non-8-en-1-ylcyclohexane (43). General procedure F was used to couple **42** (2.48 g, 9.88 mmol) and cyclohexylmagnesium chloride (2 M solution in Et_2O) to yield the title compound. 60%. Clear and colorless oil. R_f = 0.95 (hexanes; $KMnO_4$). ^{1}H NMR (500 MHz, $CDCl_3$) δ 5.84 (tt, *J* = 8.8, 6.7 Hz, 1H), 5.08 – 4.91 (m, 2H), 2.33 – 0.62 (m, 25H). ^{13}C NMR (126 MHz, $CDCl_3$) δ 138.97, 114.08, 43.54, 37.77, 37.66, 33.90, 33.53, 30.23, 29.78, 29.66, 29.04, 26.95, 26.84, 26.52.

4-(9-cyclohexylnonyl)benzaldehyde (44). General procedure D was used to couple **43** (900 mg, 4.32 mmol) and 4-bromobenzaldehyde to yield the title compound. 92%. Clear and colorless oil. R_f = 0.67 (10% EtOAc in hexanes; Seebach's Dip). ^{1}H NMR (300 MHz, $CDCl_3$) δ 9.96 (s, 1H), 7.78 (d, *J* = 8.1 Hz, 2H), 7.32 (d, *J* = 7.9 Hz, 2H), 2.67 (t, *J* = 7.7 Hz, 2H), 2.13 – 0.58 (m, 27H). ^{13}C NMR (75 MHz, $CDCl_3$) δ 192.05, 150.63, 134.63, 130.07, 129.25, 43.69, 37.81, 36.45, 33.70, 31.33, 30.40, 30.22, 29.92, 29.79, 29.70, 29.51, 27.13, 27.02, 26.70.

(*S*)-1-(4-(9-cyclohexylnonyl)benzoyl)pyrrolidine-2-carbonitrile (46). General procedure K was used to convert **44** (536 mg, 1.77 mmol) to is corresponding carboxylic acid **45**, which was taken on to the next reaction crude. General procedure I was then used to convert the crude carboxylic acid to its acid chloride and was used immediately after purification. Seperately, general procedure N was use to deprotect **34** (431 mg, 2.2 mmol). General procedure B was used to couple the deprotected **34** and **45** to yield the title compound. 83% over 2 steps. While solid. R_f = 0.61 (40% EtOAc in hexanes;

Seebach's Dip). ^{1}H NMR (500 MHz, $CDCl_3$) δ 7.47 (d, *J* = 7.0 Hz, 2H), 7.23 (d, *J* = 7.0 Hz, 2H), 4.85 (s, 1H), 3.79 – 3.44 (m, 2H), 2.60 (t, *J* = 7.3 Hz, 2H), 2.48 – 1.85 (m, 4H), 1.85 – 1.43 (m, 6H), 1.45 – 0.52 (m, 21H). ^{13}C NMR (126 MHz, $CDCl_3$) δ 169.89, 146.19, 132.25, 128.38, 127.62, 118.77, 49.51, 46.84, 37.64, 37.54, 35.82, 33.44, 31.18, 29.96, 29.66, 29.55, 29.46, 29.22, 27.02, 26.96, 26.85, 26.76, 26.44.

(*S*)-1-(4-(9-cyclohexylnonyl)benzoyl)pyrrolidine-2-carboximidamide hydrochloride (47). General procedure A was used to convert **46** (215 mg, 0.526 mmol) to the title compound. 84%. White solid. ^{1}H NMR (500 MHz, DMSO) δ 9.11 (s, 2H), 8.87 (s, 2H), 7.62 (d, *J* = 7.9 Hz, 2H), 7.25 (d, *J* = 7.8 Hz, 2H), 4.61 (t, *J* = 7.3 Hz, 1H), 4.04 – 3.66 (m, 1H), 3.43 (m, 1H), 2.70 – 2.54 (m, 2H), 2.37 (d, *J* = 6.1 Hz, 1H), 2.03 – 1.77 (m, 3H), 1.77 – 1.45 (m, 6H), 1.45 – 0.65 (m, 21H). ^{13}C NMR (126 MHz, DMSO) δ 171.56, 169.93, 145.60, 133.21, 128.38, 128.30, 58.49, 50.66, 37.48, 37.41, 35.44, 33.36, 31.40, 31.19, 29.80, 29.49, 29.42, 29.28, 29.09, 26.70, 26.32, 25.68. LCMS: t_R = 6.01; m/z = 426.3. HRMS m/z calc. for $C_{27}H_{44}N_3O$ (M+H), 426.3484; found, 426.3475.

4a ^{1}H NMR (300 MHz, DMSO)

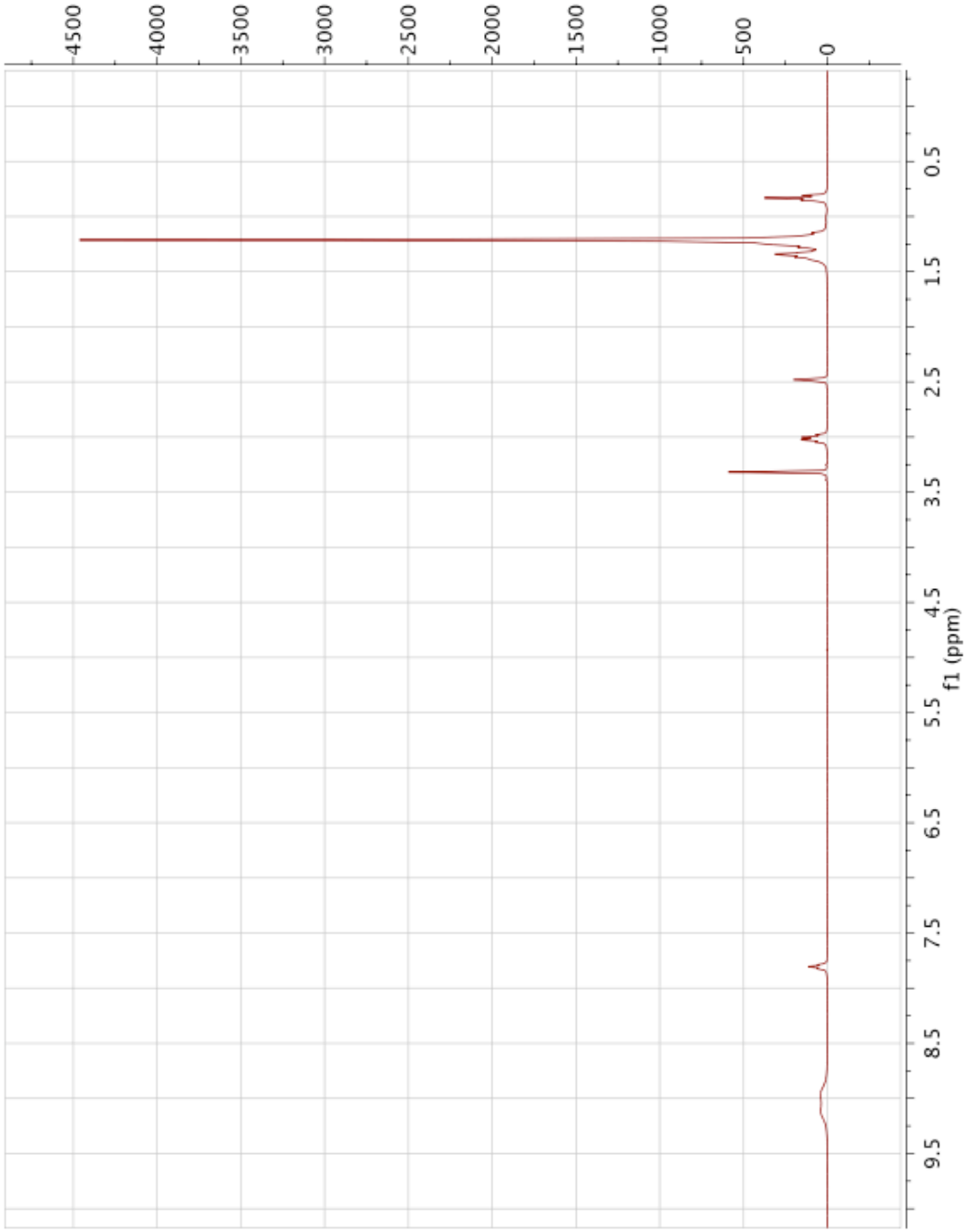

4a ^{13}C NMR (75 MHz, DMSO)

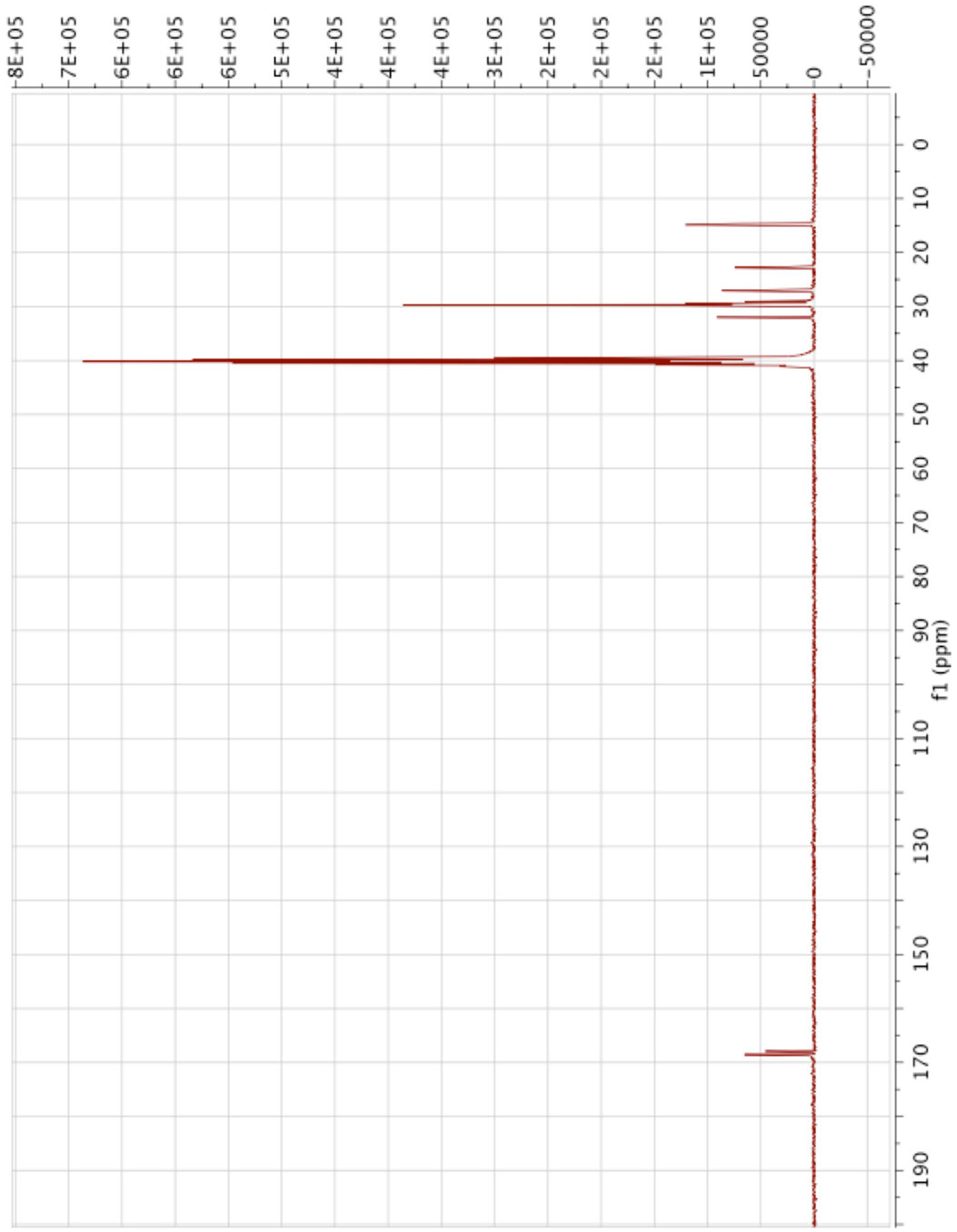

9c ^{1}H NMR (300 MHz, DMSO)

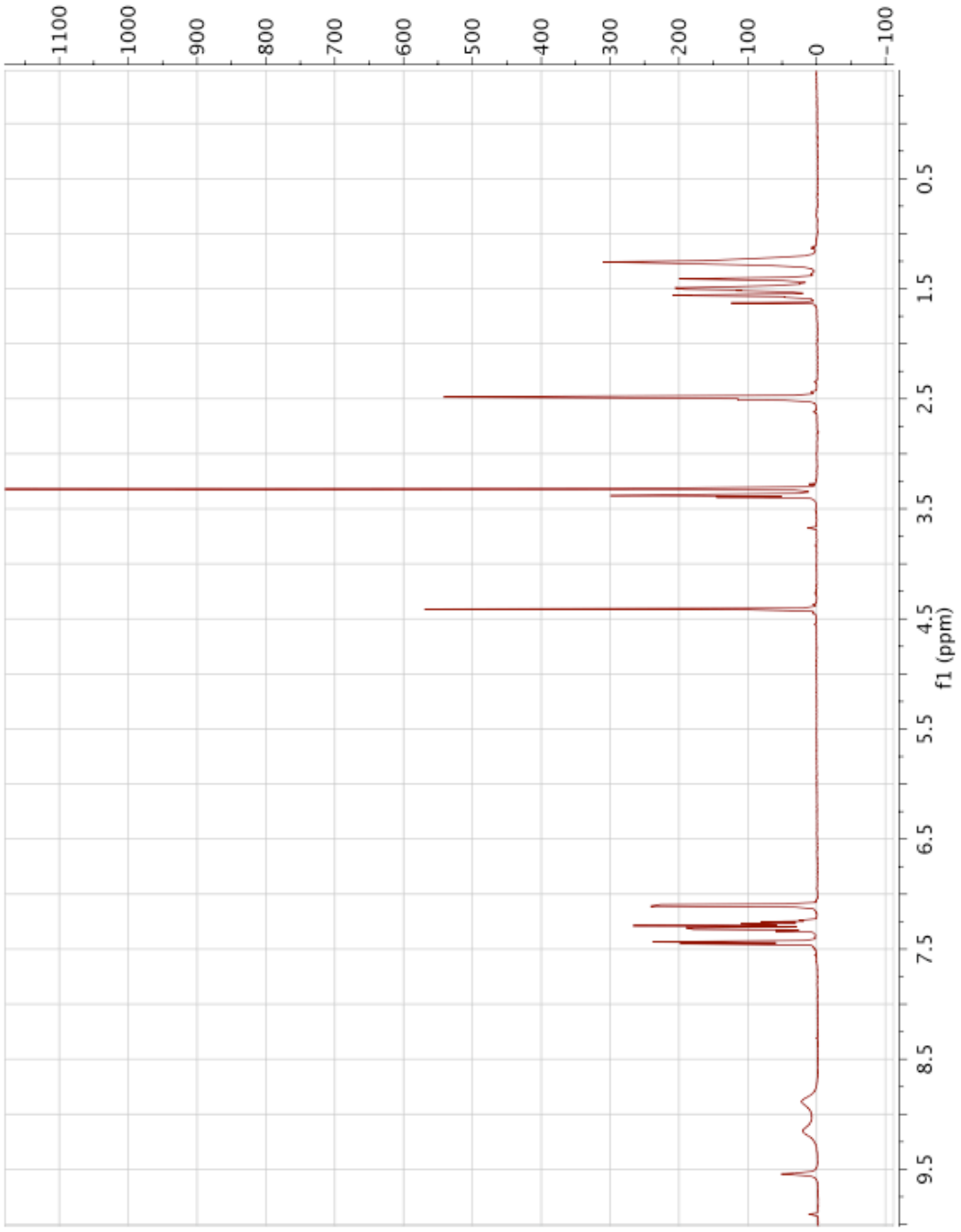

9c ^{13}C NMR (75 MHz, DMSO)

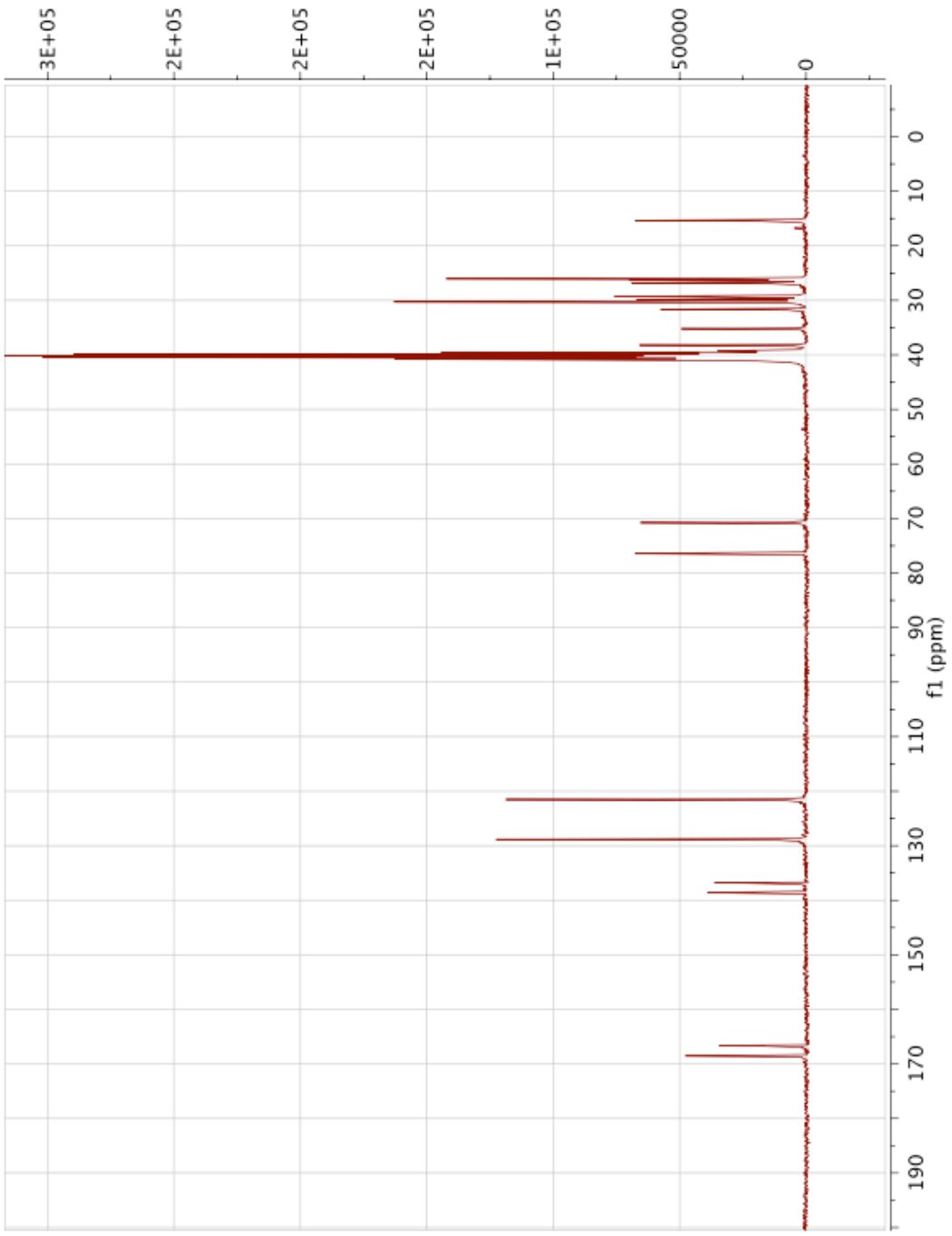
3E+05
2E+05
2E+05
2E+05
1E+05
50000
0
0
10
20
30
40
50
60
70
80
90
110
130
150
170
190
f1 (ppm)

14a ^{1}H NMR (500 MHz, DMSO)

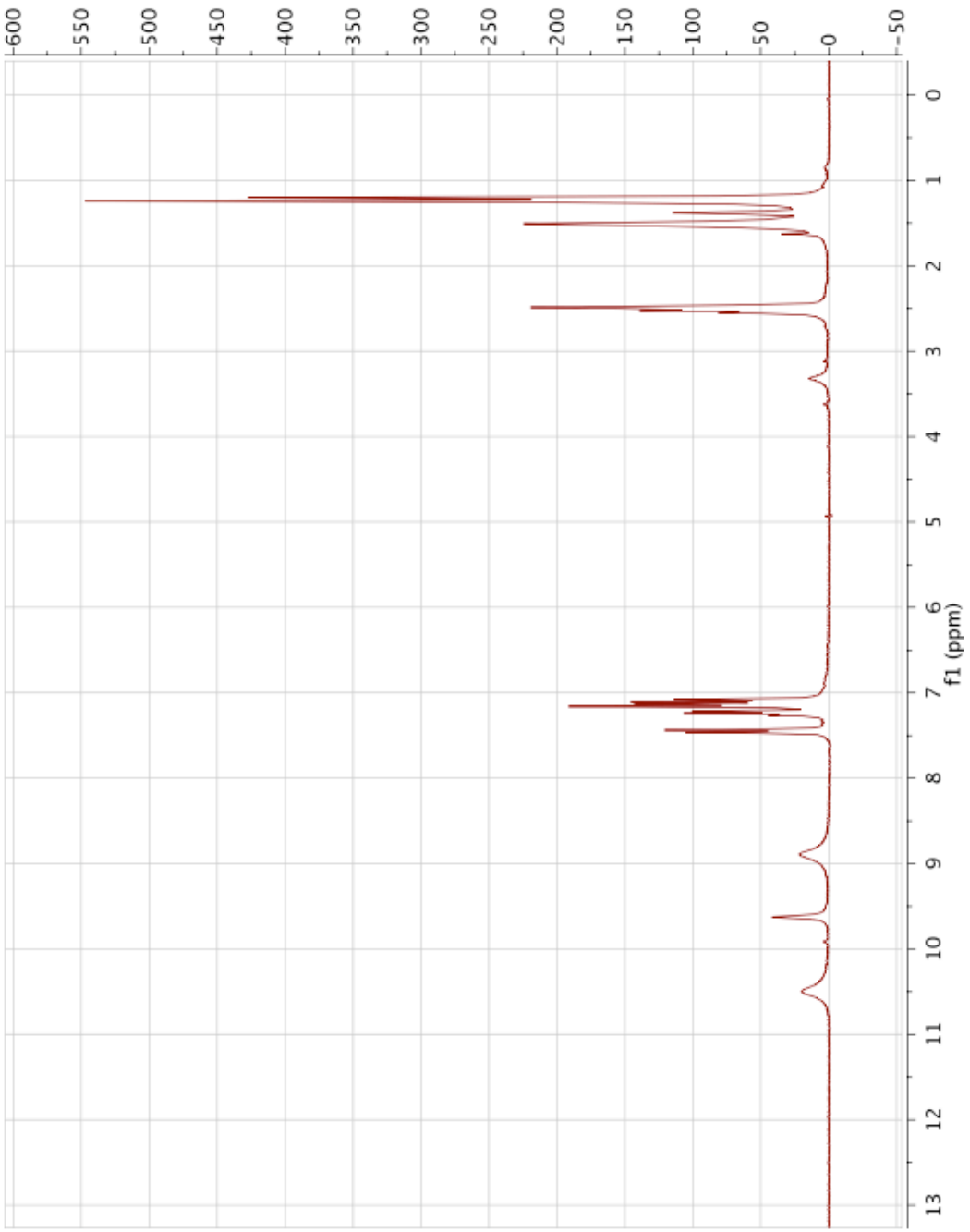

14a ^{13}C NMR (126 MHz, DMSO)

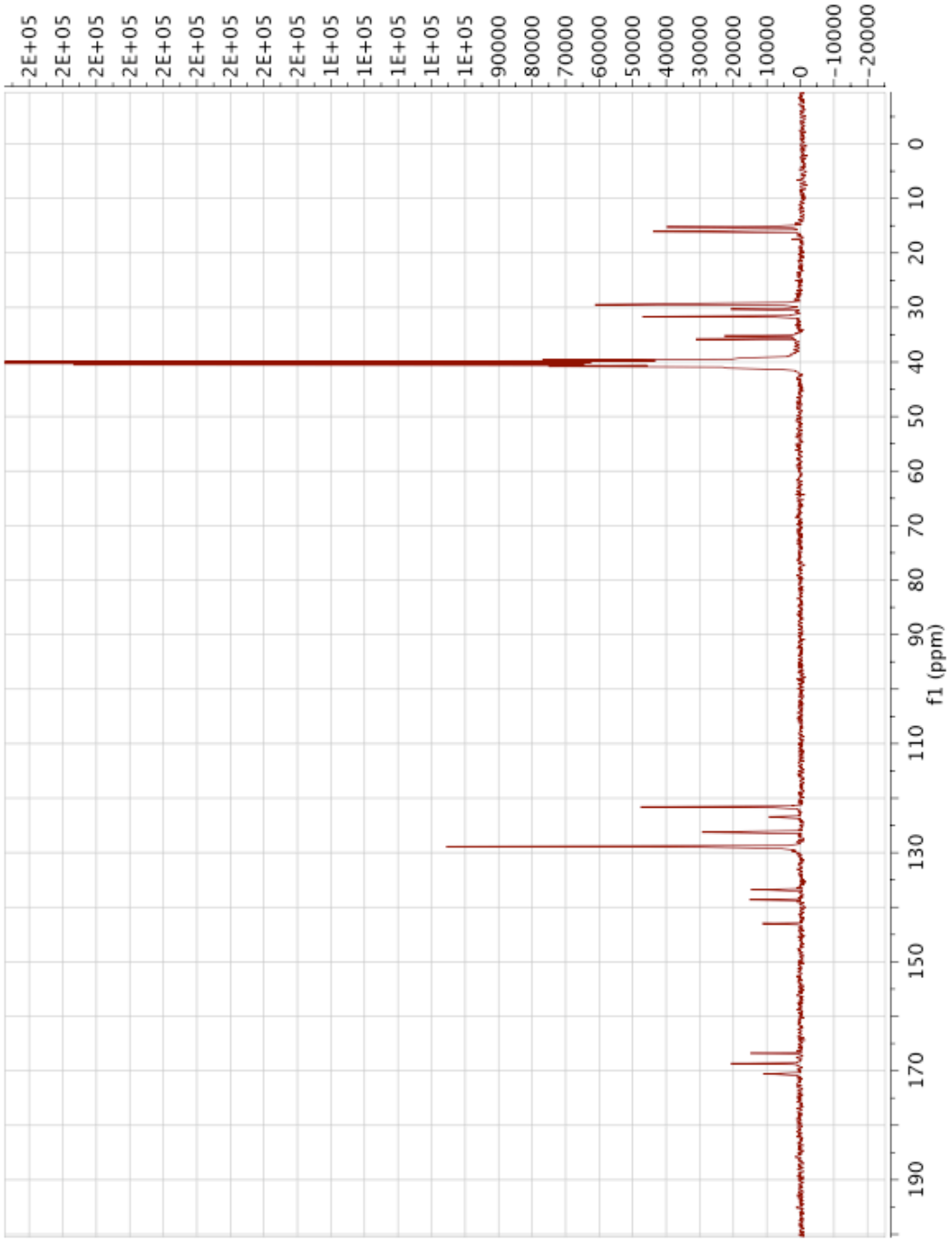

19a ^{1}H NMR (500 MHz, DMSO)

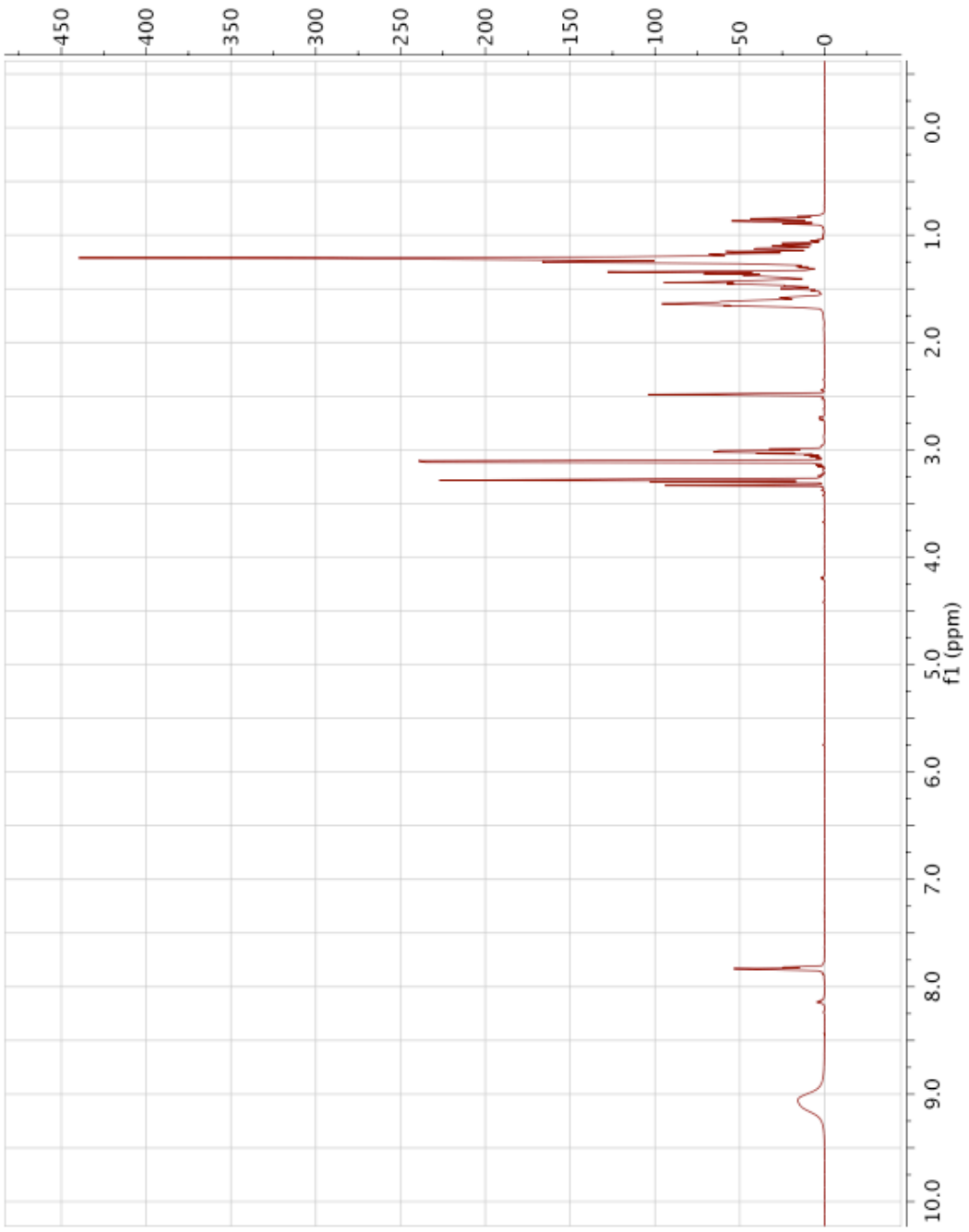

19a ^{13}C NMR (126 MHz, DMSO)

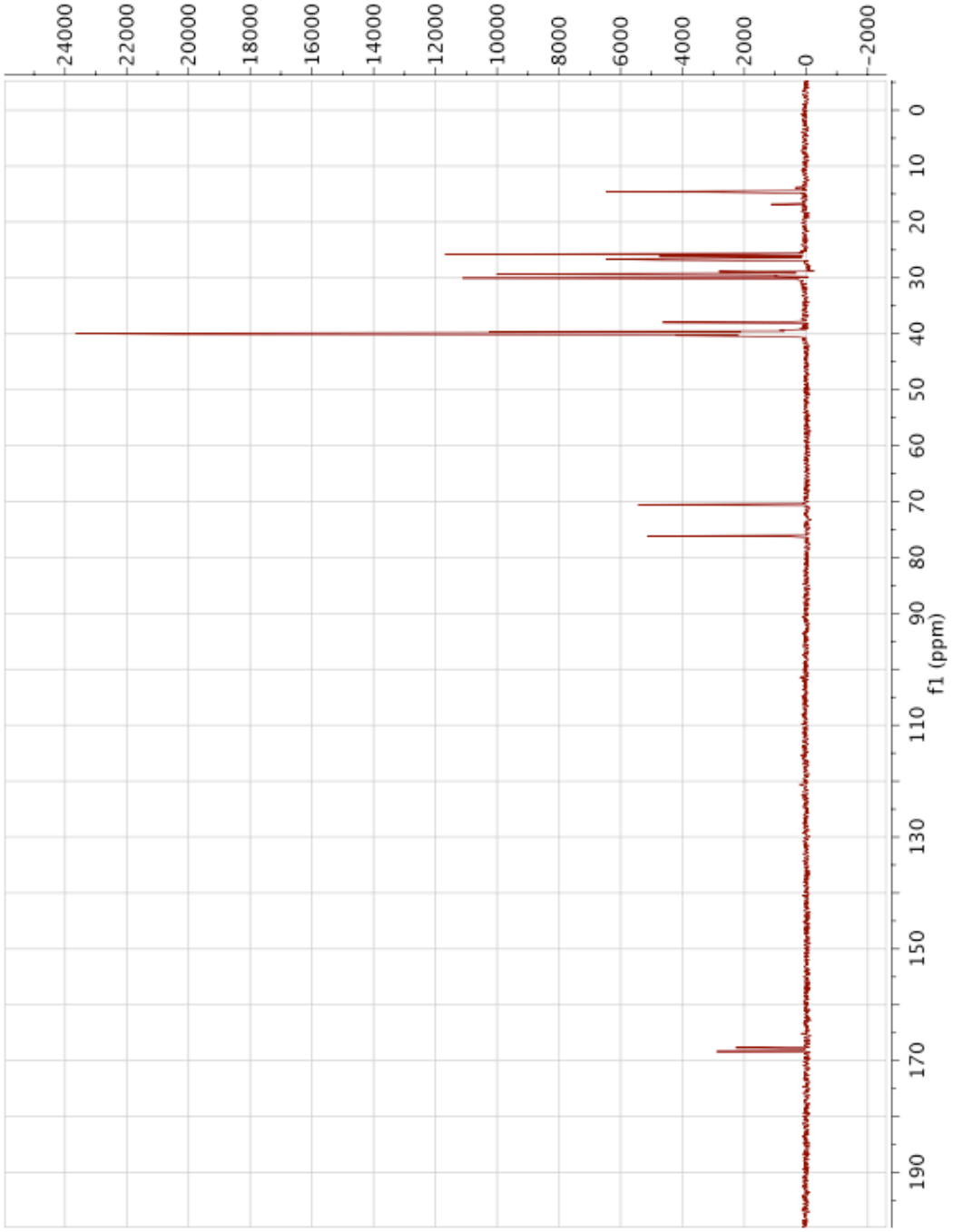

23b ^{1}H NMR (500 MHz, DMSO)

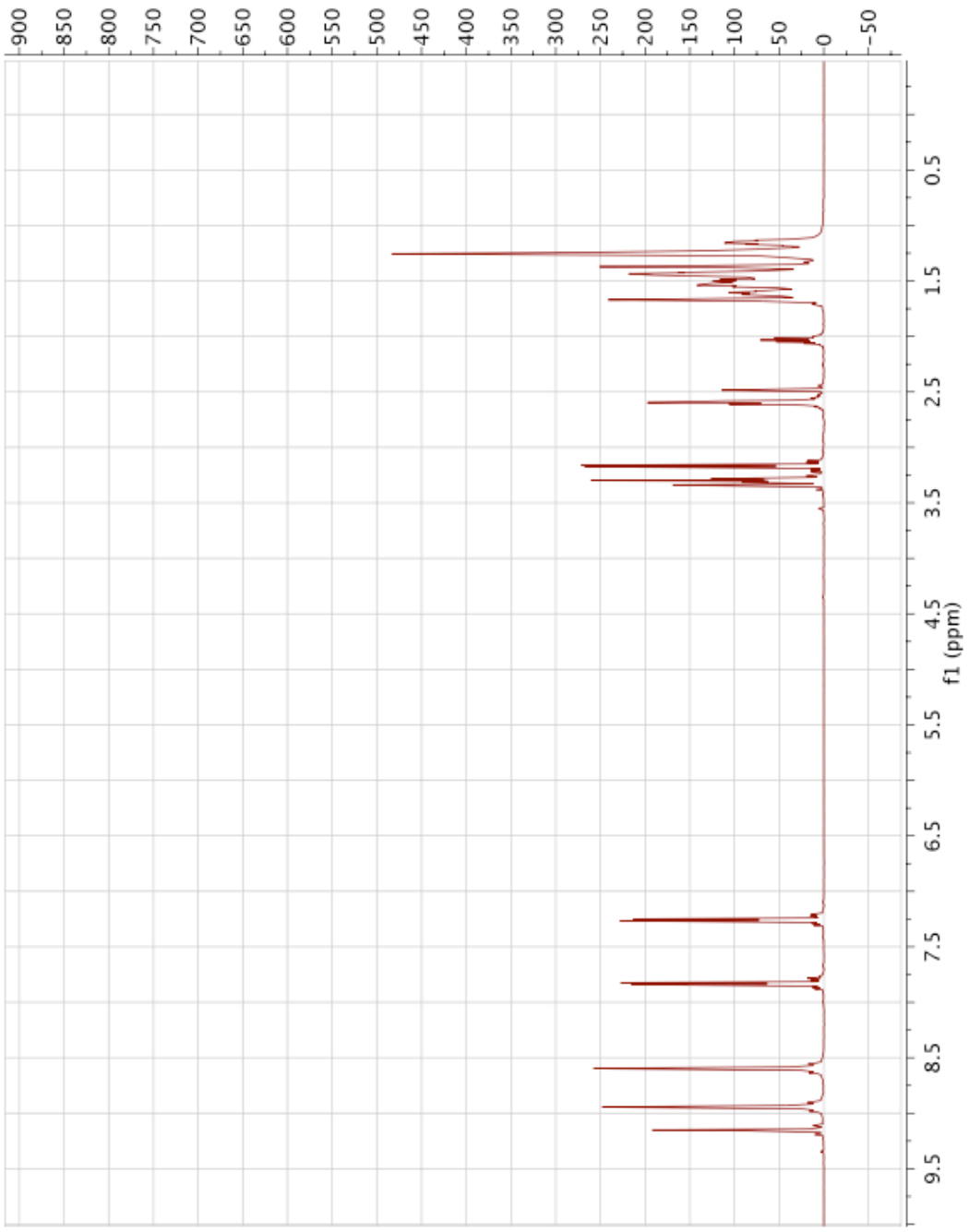

23b ^{13}C NMR (126 MHz, DMSO)

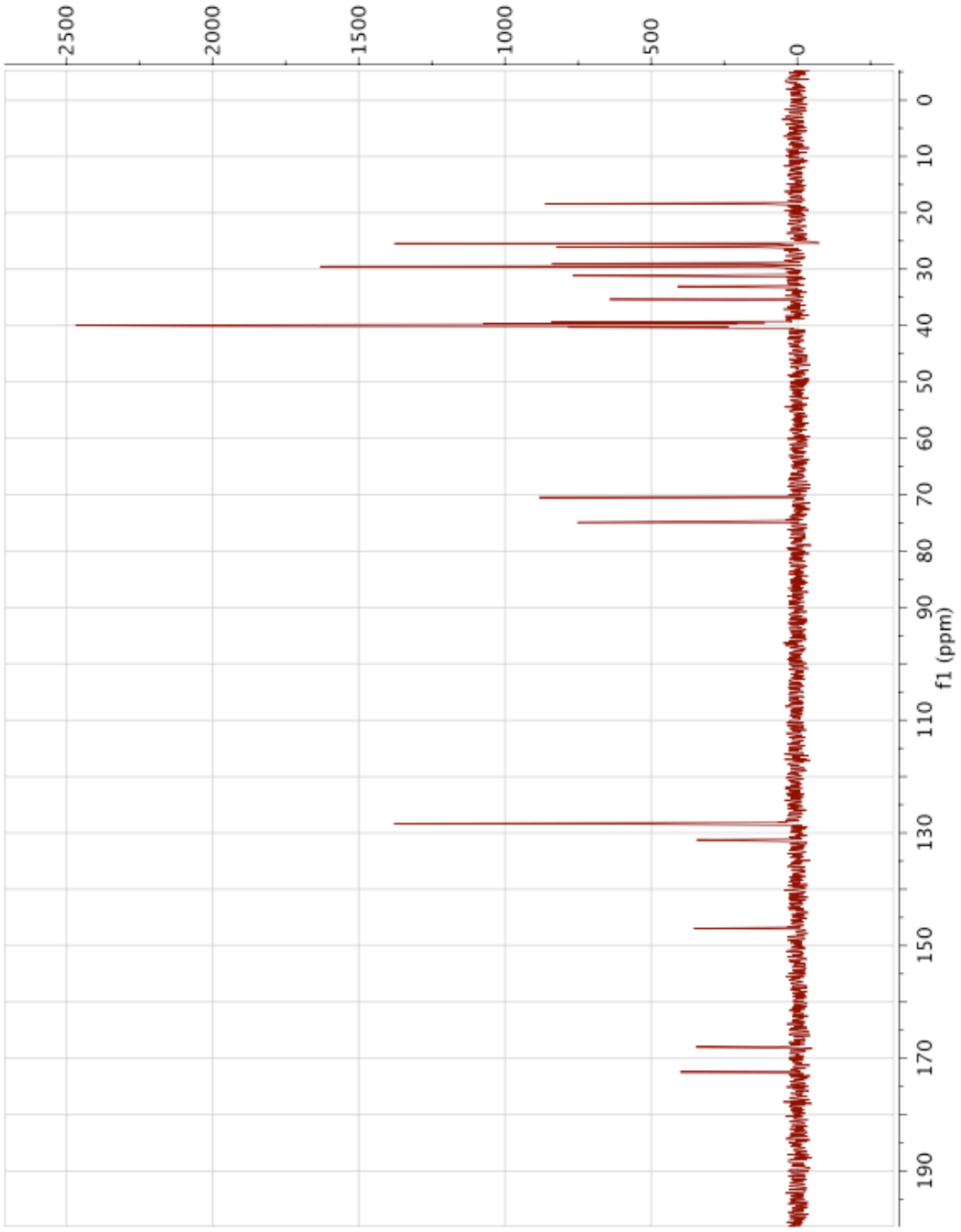

33 ^{1}H NMR (500 MHz, DMSO)

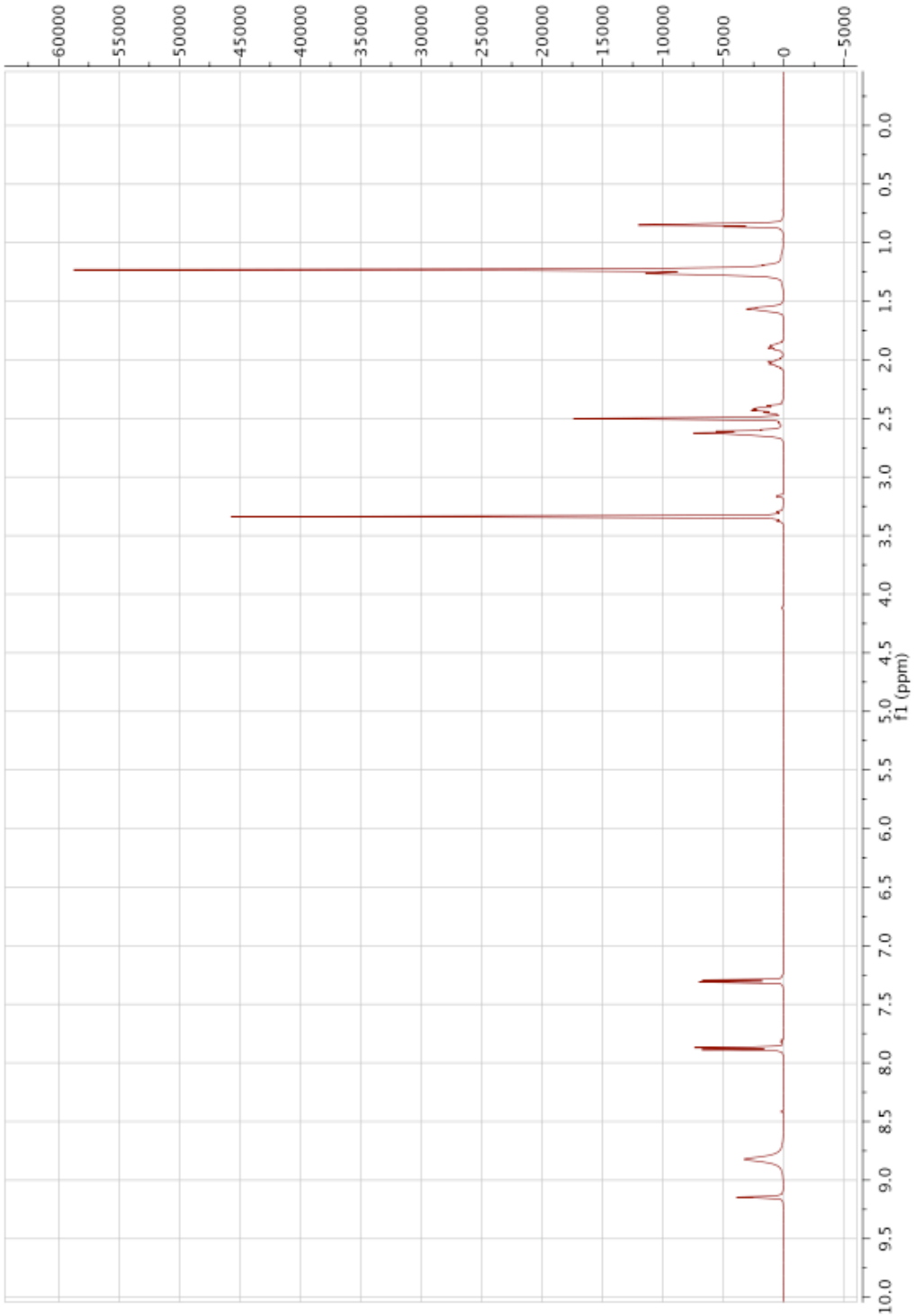

33 ^{13}C NMR (126 MHz, DMSO)

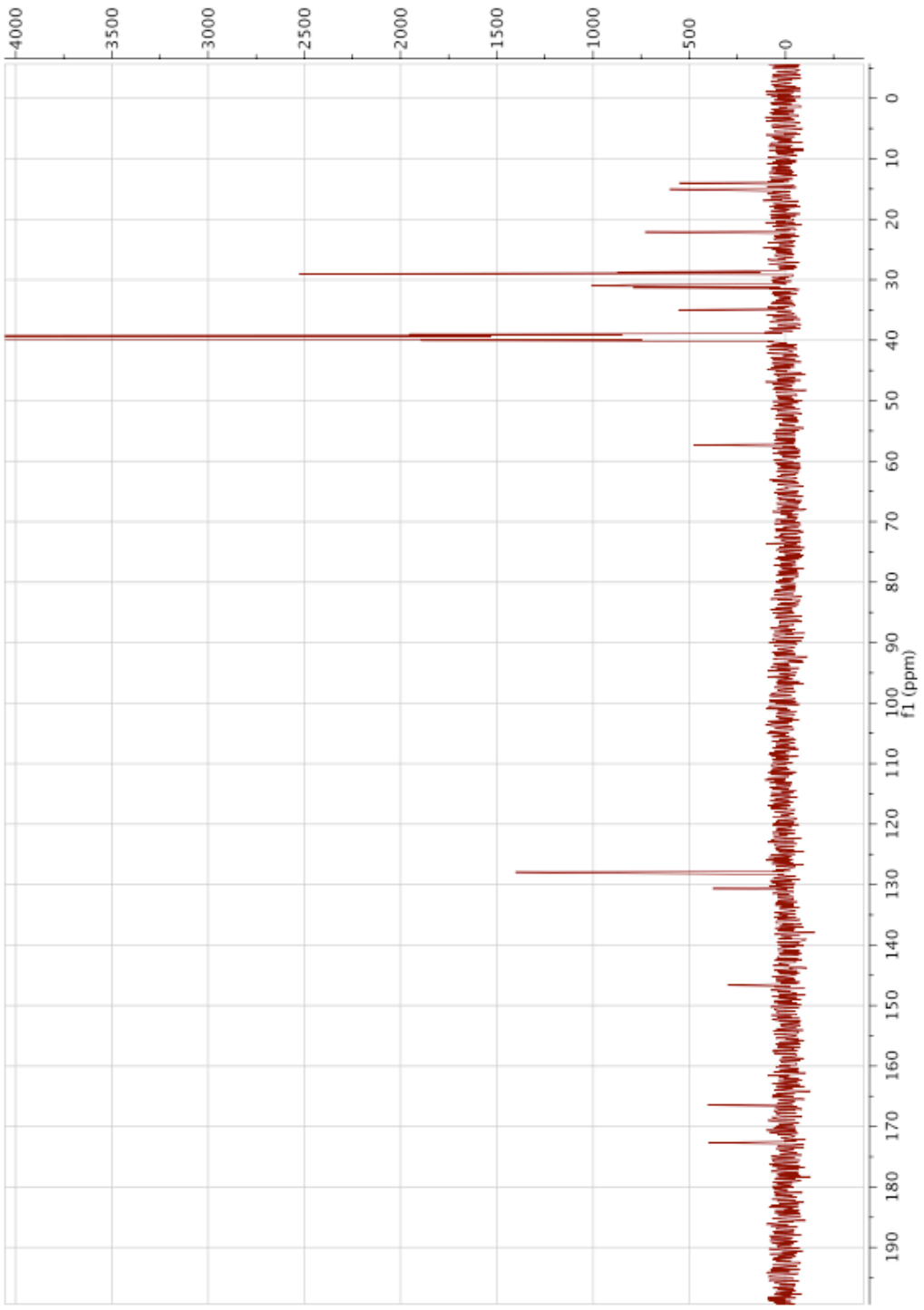

38 ^{1}H NMR (500 MHz, DMSO)

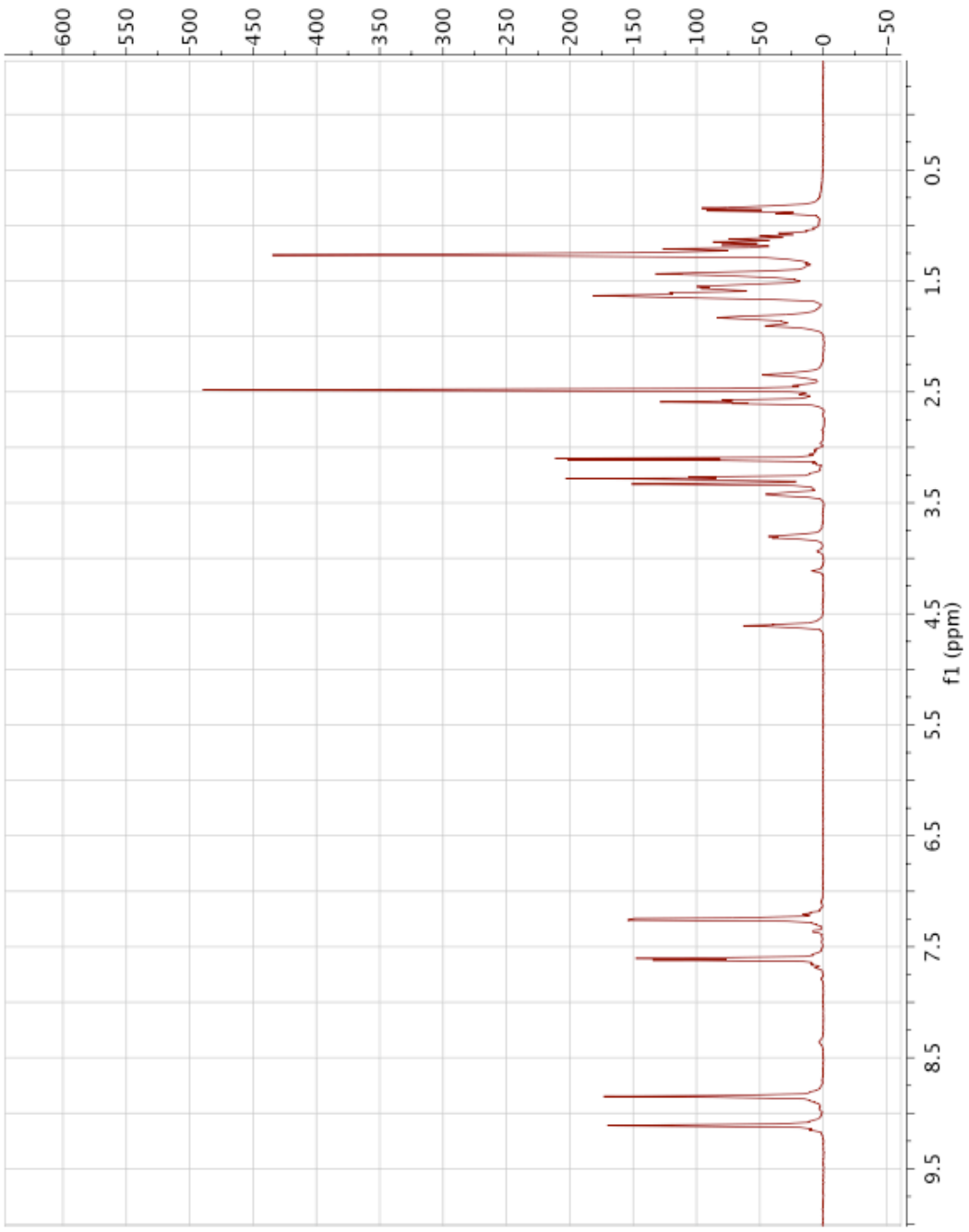

38 ^{13}C NMR (126 MHz, DMSO)

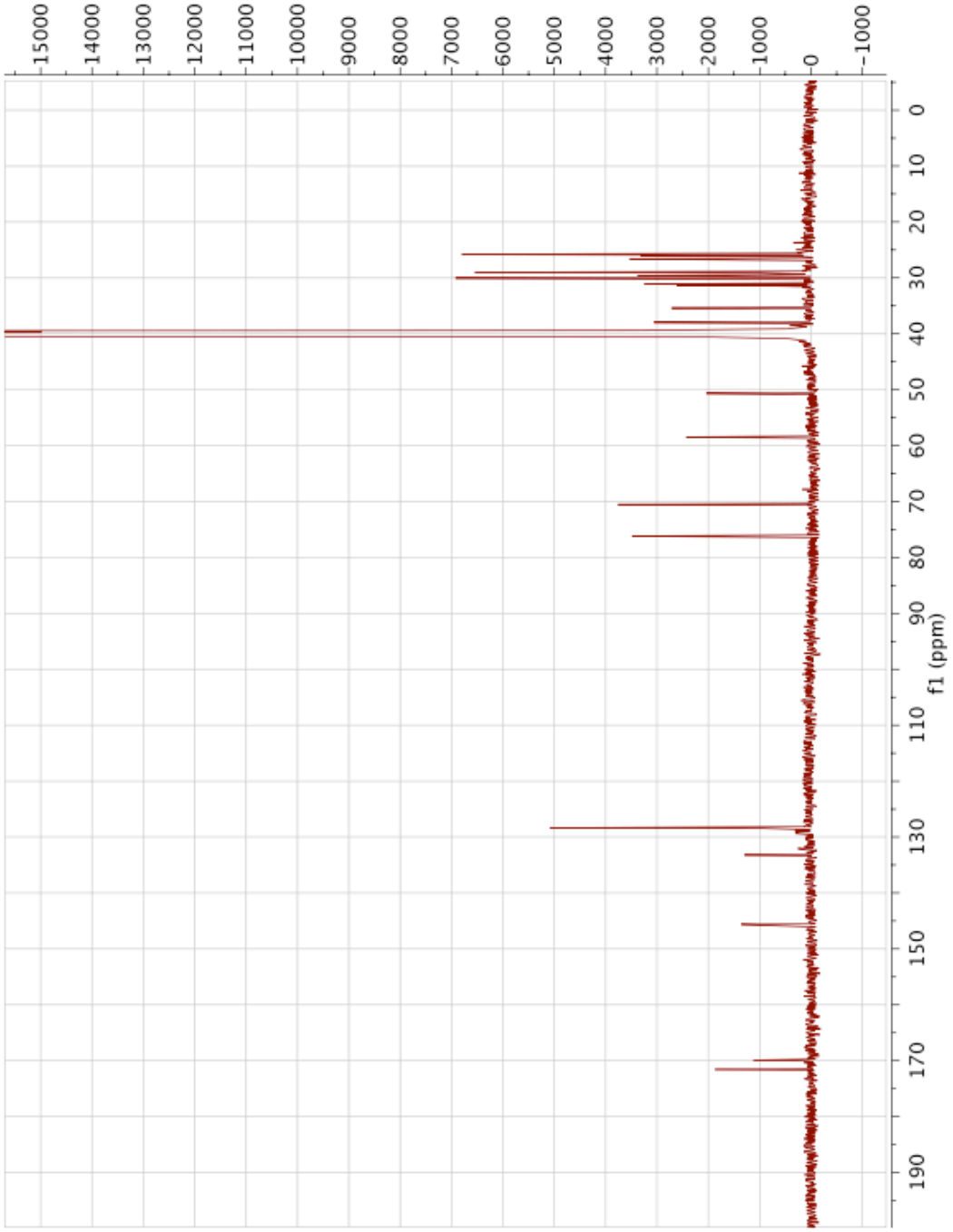

56 ^{1}H NMR (500 MHz, DMSO)

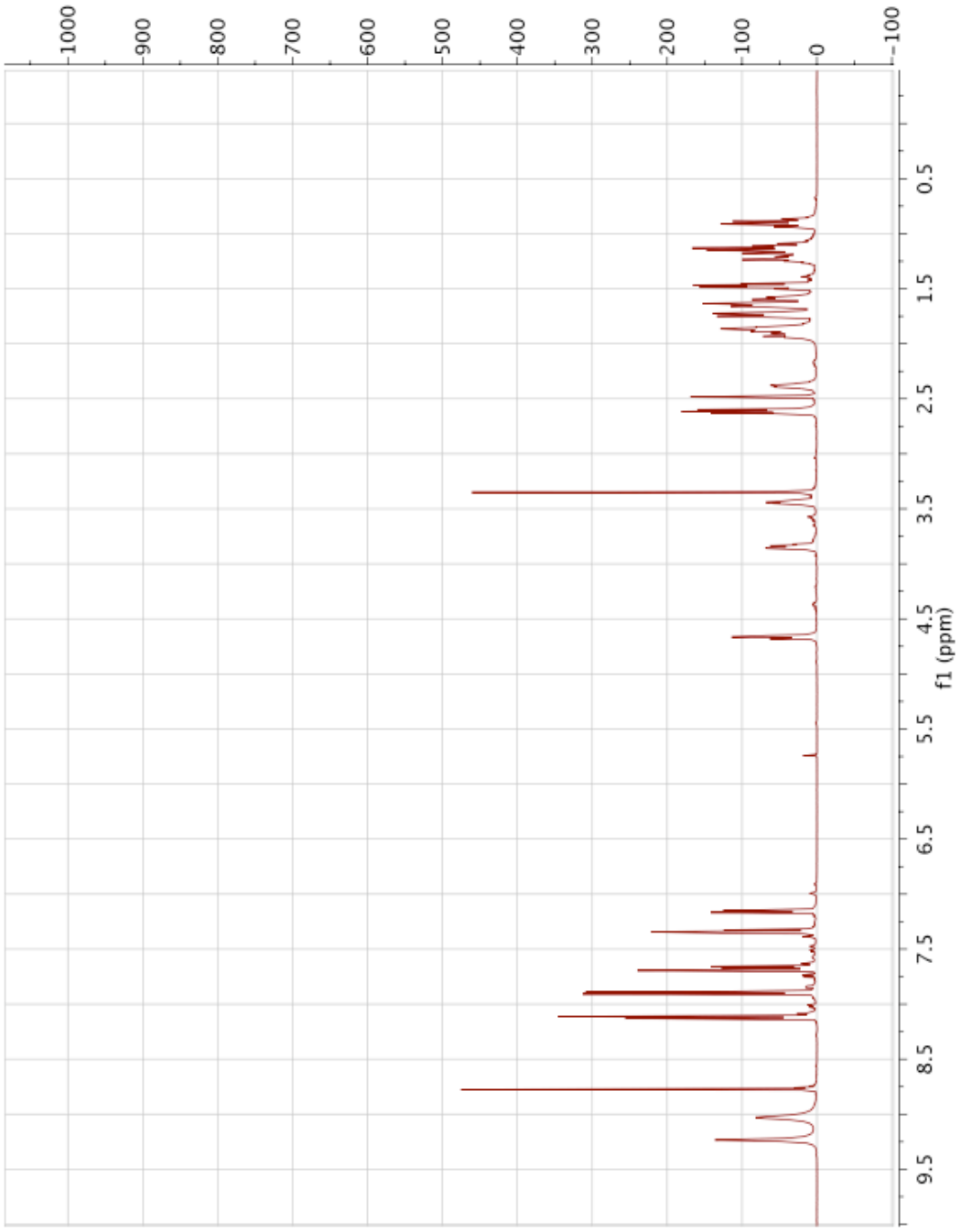

56 ^{13}C NMR (126 MHz, DMSO)

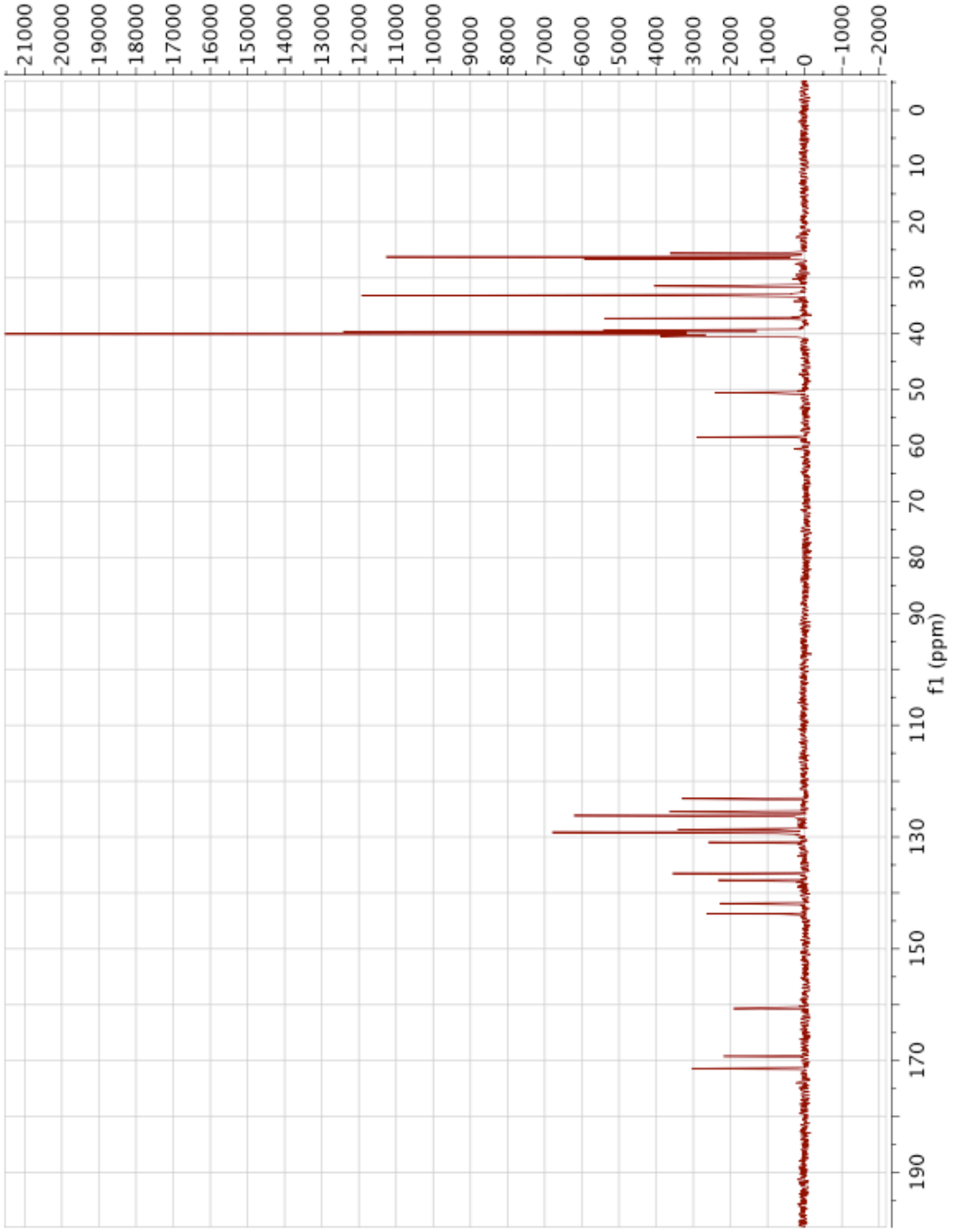

SI References

1. Miller, D. J.; Jerga, A.; Rock, C. O.; White, S. W. Analysis of the staphylococcus aureus dgkb structure reveals a common catalytic mechanism for the soluble diacylglycerol kinases. *Structure* **2008,** 16, 1036-1046.
2. Hirosawa, M.; Totoki, Y.; Hoshida, M.; Ishikawa, M. Comprehensive study on iterative algorithms of multiple sequence alignment. *Comput Appl Biosci* **1995,** 11, 13-18.
3. Chemical Computing Group, I. *Molecular operating environment (moe)*, MOE 2009.10.
4. Pitson, S. M.; Moretti, P. A. B.; Zebol, J. R.; Lynn, H. E.; Xia, P.; Vadas, M. A.; Wattenberg, B. W. Activation of sphingosine kinase 1 by erk1/2-mediated phosphorylation. *EMBO J* **2003,** 22, 5491-5500.
5. Cabrera, R.; Ambrosio, A. L. B.; Garratt, R. C.; Guixé, V.; Babul, J. Crystallographic structure of phosphofructokinase-2 from escherichia coli in complex with two atp molecules. Implications for substrate inhibition. *J Mol Biol* **2008,** 383, 588-602.
6. Cabrera, R.; Baez, M.; Pereira, H. M.; Caniuguir, A.; Garratt, R. C.; Babul, J. The crystal complex of phosphofructokinase-2 of escherichia coli with fructose-6-p: Kinetic and structural analysis of the allosteric atp inhibition. *J Biol Chem* **2010**.
7. Wildman, S.; Crippen, G. Prediction of physicochemical parameters by atomic contributions. *Journal of chemical information and computer sciences* **1999,** 39, 868-873.